Optical-mechanical properties of diseased cells measured by interferometry

Natan T. Shaked,
Y. Bishitz, H. Gabai, and P. Girshovitz

Department of Biomedical Engineering, Faculty of Engineering
Tel Aviv University, Ramat Aviv 69978, Israel

ABSTRACT

Interferometric phase microscopy (IPM) enables to obtain quantitative optical thickness profiles of transparent samples, including live cells *in-vitro*, and track them in time with sub-nanometer accuracy without any external labeling, contact or force application on the sample. The optical thickness measured by IPM is a multiplication between the cell integral refractive index differences and its physical thickness. Based on the time-dependent optical thickness profile, one can generate the optical thickness fluctuation map. For biological cells that are adhered to the surface, the variance of the physical thickness fluctuations in time is inversely proportional to the spring factor indicating on cell stiffness, where softer cells are expected fluctuating more than more rigid cells. For homogenous refractive index cells, such as red blood cells, we can calculate a map indicating on the cell stiffness per each spatial point on the cell. Therefore, it is possible to obtain novel diagnosis and monitoring tools for diseases changing the morphology and the mechanical properties of these cells such as malaria, certain types of anaemia and thalassemia. For cells with a complex refractive-index structure, such as cancer cells, decoupling refractive index and physical thickness is not possible in single-exposure mode. In these cases, we measure a closely related parameter, under the assumption that the refractive index does not change much within less than a second of measurement. Using these techniques, we lately found that cancer cells fluctuate significantly more than healthy cells, and that metastatic cancer cells fluctuate significantly more than primary cancer cells.

Keywords: Interferometric phase microscope, holography, cell imaging.

1. INTRODUCTION

Interferometric phase microscopy (IPM) provides unique advantages over conventional bright-field microscopy, having the possibility to record the optical thickness map of the sample without external labeling[1]. The optical thickness measured by IPM is a multiplication between the cell integral refractive index differences and its physical thickness per each of the sample spatial points. Using the time-dependent optical thickness profile, one can generate the optical thickness fluctuation map, indicating on rigidity of each of the cells in the field of view, which is useful for characterizing various diseases. For example, it was shown that wide-field IPM is useful for characterizing the cell stiffness changes in sickle cell disease[2] and in cancer[3].

As opposed to atomic force microscope (AFM) or other force applying methods providing mechanical measurements of cells, IPM is a noncontact and completely nonintrusive technique that is able to record the entire complex wave-front (amplitude and phase) of the light which has interacted with the sample *in-vitro* by using a low-power coherent or partially-coherent light source, where no exogenous labelling or special sample preparations are involved.

Using IPM, the quantitative phase profile of the sample is obtained by first capturing the interference between a beam going through the sample and a mutually-coherent reference beam that does not interact with the sample. The creation of interference pattern on the digital camera is possible using conventional interferometric setups, such as the ones based on Mach-Zehnder or Michelson interferometers, or using compact, portable, and easy-to-align interferometers that are more stable due to their common-path geometry[4-6]. The digital process is chosen according to the setup used. After the digital process applied on the acquired interferogram, the phase profile of the interferogram acquired at time t is defined as follows[7]:

$$\phi(x,y;t) = \frac{2\pi}{\lambda}[(\bar{n}_c(x,y;t) - n_m) \times h_c(x,y;t) + n_m h_m], \tag{1}$$

where λ is the illumination wavelength, h_m is the thickness of the cell growth medium, n_m is the refractive index of the medium, h_c is the thickness profile of the cell, and $\bar{n}_c$ is the cell integral refractive index which is defined as follows:

$$\bar{n}_c(x,y;t) = \frac{1}{h_c(x,y;t)} \int_0^{h_c(x,y;t)} n_c(x,y,z;t)dz. \tag{2}$$

We then define the standard deviation of the time-dependent phase profile as follows:

$$STD(x,y) = \sqrt{\left\langle \phi(x,y;t)^2 \right\rangle_t - \left\langle \phi(x,y;t) \right\rangle_t^2} \tag{2}$$

where $\langle \bullet \rangle_t$ denotes time average.

For biological cells that are adhered to the surface, the standard deviation indicates on cell stiffness, where softer cells are expected fluctuating more than more rigid cells. For homogenous refractive index cells such as red blood cells, the standard deviation square is inversely proportional to the effective spring constant, which is related to the in-plane shear modulus of the cell[8]. Therefore, $STD(x,y)$ represents a map indicating on the cell stiffness per each spatial point on the cell, using which it is possible to obtain novel diagnosis and monitoring tools for diseases changing the morphology and the mechanical properties of the cells such as malaria[8], certain types of anaemia[2] and thalassemia.

For cells with a complex refractive-index structure, such as cancer cells, decoupling refractive index and physical thickness is not possible in single-exposure mode. In these cases, we measure a closely related parameter, under the assumption that the refractive index does not change much within less than a second of measurement.

2. EXPERIMENTAL RESULTS

In Ref. (3), we have performed IPM measurements on cancer and healthy cells in order to establish a cancer biomarker based on the unique optical-mechanical signatures of cancer cells measured in a noncontact, label-free manner by IPM.

Cell stiffness is a relatively new biomarker for cancer. Lately, it has been shown using AFM that cancer cells are nearly four times softer than similar but healthy cells[9]. Although the contribution of the cell mechanical properties in invasion is not completely clear, it is possible that greater elasticity of cancer cells helps them metastasize by more easily squeezing through the body tissues and capillaries[10-13].

Stiffness as a cancer biomarker is important for preventing false diagnosis using the conventional and subjective cancer identification that is currently performed under a regular optical microscope. However, AFM is expensive, hard to implement, and applies forces on the cell measured. In addition, AFM measurement alone can yield a wrong diagnosis, since cells might be less rigid due to reasons other than cancer. For these reasons, IPM has higher clinical potential for measurements of the mechanical properties of cancer cells.

For a valid comparison of the mechanical features of two types of cells, it is highly important that the cells are taken from the same donor and originated in the same organ. Cells from various organs or different donors have high variability of mechanical properties. The *in-vitro* model used in the study presented in Ref. (3) is consisted of two pairs of cell lines. The first pair of cell lines includes normal rat enterocytes named IEC-18 (non-transformed small Intestinal Epithelial Cells) as the control group, and cancer-transformed rat enterocytes (named R1, or IEC-18 Ras) as the experimental group, both taken from the exact same source – certain rat intestinal epithelium. When the two types of cells were infused into healthy rats, only those rats that received the modified cancerous cells developed tumors[14-17]. Next, to measure the mechanical changes during metastasis, we used the SW-480 cell line derived from a primary human colorectal carcinoma, and the SW-620 cell line, containing colorectal adenocarcinoma cells derived from a lymph node metastasis of the same patient[18,19].

For the IPM measurements, we implemented a portable, off-axis, common-path and low-coherence interferometric modules that can be easily connected at the output of a regular transmission microscope illuminated by a coherent or

partially coherent source, and transform it into a powerful IPM system without special optical expertise or meticulous alignment, while tracking the optical thickness profiles with sub-nanometer sensitivity. These interferometers are suitable to be used outside of the vibration-isolated environment of an optical lab, and in clinics. Since the beams in these setups interfere with an angle (off-axis geometry), the optical thickness profile of the sample can be reconstructed using a single interferogram, and thus fast acquisition rate is possible. To obtain the time dependent phase profile defined in Eq. (1), per each interferograms the digital process includes a spatial filtering of one of the cross-correlation orders, taking its phase argument in the image domain, applying a phase unwrapping algorithm to solve 2π ambiguities and wave front curvature compensation[1]. Using the resulting quantitative phase profile, the optical thickness profile is achieved by division with $2\pi/\lambda$, where λ is the central wavelength of the illuminating light source.

The first experimental comparison was carried out on the rat intestinal epithelial cell lines: healthy cells (IEC-18) and cancer-transformed cells (R1). For each cell in each group, we captured a series of 100 off-axis interferograms per second, one of which is shown for a healthy cell in Fig. 1(a). After applying the digital off-axis interferometric process
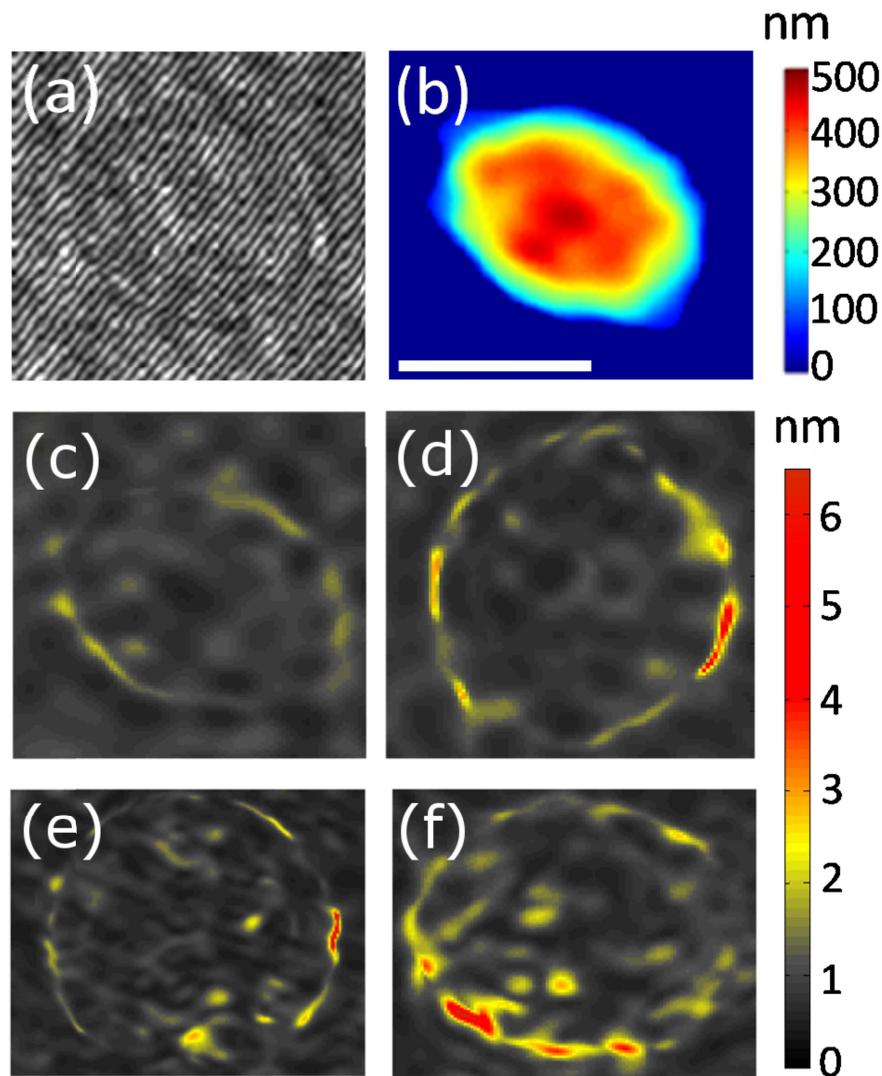
Figure 1. Wide-field IPM imaging of rat intestinal epithelial cells (a-d) and human colorectal carcinoma cells (e,f). (a) Off-axis interferogram of a healthy cell (IEC-18). (b) Quantitative optical thickness profiles of the IEC-18 cell. (c) Fluctuation STD maps of the IEC-18 cell. (d) Fluctuation STD maps of an R1 cancer cell. (e) Fluctuation STD map of an SW-480 primary cancer cell. (f) Fluctuation STD map of an SW-620 metastatic cancer cell. White scale-bar represents 10 μm. Colorbars represent optical thickness and optical thickness fluctuation STD in nanometers. Figure is from Ref. (3).

described above and subtracting the average of the background of optical thickness profile, we obtained the final quantitative optical thickness profile of the sample (see example in Fig. 1(b) for the healthy cell). From each series of thickness profiles obtained for each cell, we calculated fluctuation STD map (see examples in Figs. 1(c) for the healthy cell and in Figs. 1(d-f) for cancer cells). As can be seen from these figures, the edges of the cells have significantly higher fluctuations than the inside of the cells, whereas inside the cells the fluctuations were significantly higher than the level of the background (cell medium) fluctuations in several discrete areas.

The cell edges are digitally identified by a standard edge detection algorithm, which resulted in an average edge width coinciding with the spatial resolution limit. Based on this identification, we compared two assessments: fluctuations on the cell peripheral edges, and fluctuations inside the cell, where only the higher fluctuations areas are taken into consideration by choosing the maximum values of the optical thickness maps in each assessment. To validate that the fluctuations are driven by biological phenomena and not by system stability problems, we measured 15 μm polystyrene beads in water. Indeed, the fluctuation STD map in this case was all at the background level, including at the edges.

Using the process described above, we created a database of 22 rat intestinal epithelial cancer cells and 22 rat intestinal epithelial healthy cells. Fig. 2(a) shows the maximum fluctuation STD values for each assessment, where in both cases there is high statistical difference between the groups of healthy and cancer cells, as indicated by the low p
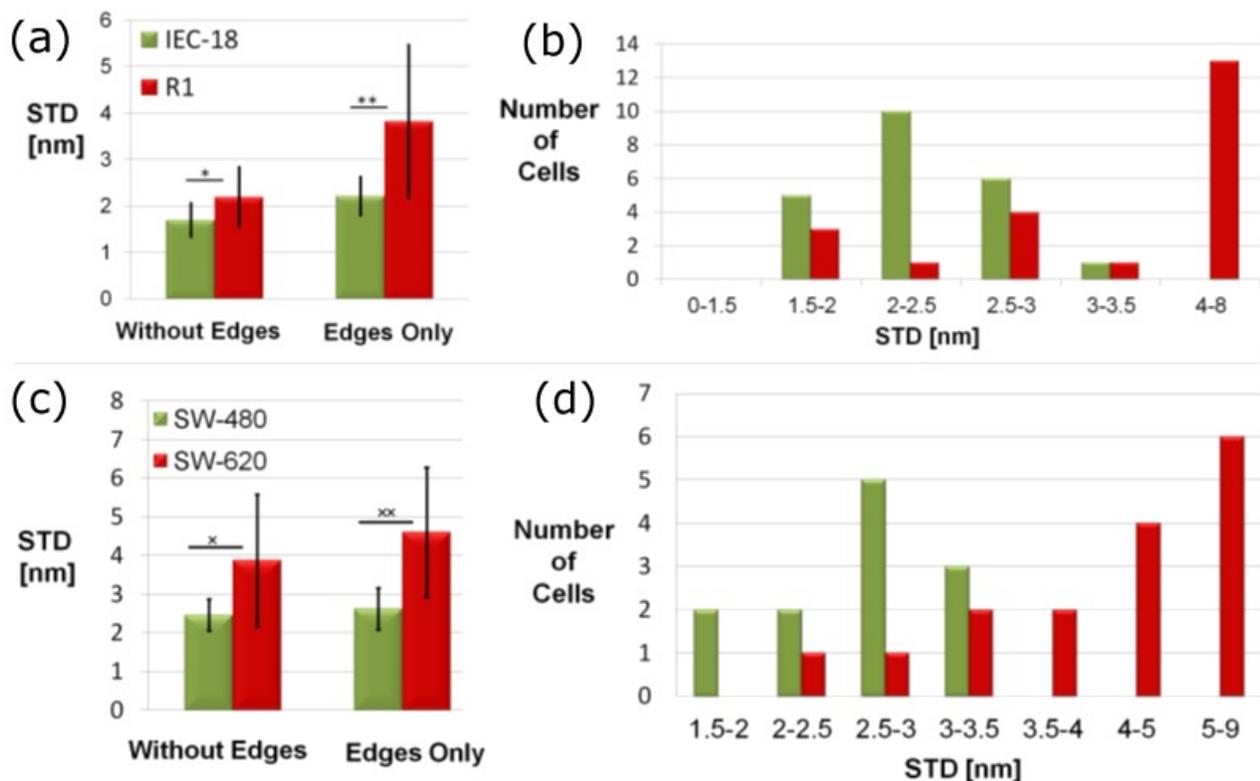
Figure 2. Results based on IPM measurements of rat intestinal epithelial healthy (IEC-18) and cancer (R1) cell lines (a,b), and human colorectal carcinoma primary cells (SW-480) and their metastatic version (SW-620) (c,d). (a) Comparison between the maximum fluctuation STD values of the healthy cells and the cancer cells for the cell inside, excluding edges, *,p<0.0025, and for the cell edges only, **,p<0.0001. (b) Distribution of the maximum fluctuation STD values taken from the entire area of each cell from both cell lines. Cancer cells fluctuated significantly more than healthy cells. (c) Comparison between the maximum fluctuation STD values of the primary cells and the metastatic cells for the inside of the cell (without edges), ×,p<0.005, and for the cell edges only, ××,p<0.0003. (d) Distribution of the maximum fluctuation STD values taken from the entire cell area (inside and edges) of each cell from both cell lines (with p<0.0003 between the groups). Metastatic cancer cells fluctuated significantly more than primary cancer cells. For comparison between cell-line groups, we used p values obtained by a standard two-tailed unpaired t-test. Figure is modified from Ref. (3).

values ($p < 0.0025$ for the inside of the cell and $p < 0.0001$ for the edges only). Figure 2(b) shows the maximum fluctuation STD distribution for the entire cell area (inside and peripheral edges together). Validation measurements were performed using AFM (see data presented in Ref. (3)).

To check the potential of IPM to yield an indication of cancer malignancy, we carried out additional measurements using IPM for human colorectal carcinoma cells (SW-480) and their metastatic version (SW-620), and analysed them by the same methods described for the rat intestinal epithelial cells. Figures 1(e) and (f) show the fluctuation STD maps of a primary cancer cell and a metastatic cancer cell, respectively. Figure 2(c) shows maximum fluctuation STD values for 16 metastatic cancer cells and 12 primary cells without the cell edge (with $p < 0.005$ between the groups) and on the edges only (with $p < 0.0003$ between the groups). Figure 2(d) shows the distribution of the maximum fluctuation STD values for the entire cell area. As can be seen from these figures, the groups of the metastatic cancer cells and of the primary cancer cells are well discriminated based on their fluctuations, where the metastatic cells fluctuate significantly more than the primary cells.

3. CONCLUSIONS

Interferometry can yield indications of cell mechanical properties by measuring the cell optical thickness fluctuations over a short period of time, where adherent cells that fluctuate more are assumed to be less stiff. Using compact and portable IPM setups, we have lately measured cancer and healthy cells and found that cancer cells fluctuate significantly more than healthy cells, and that metastatic cancer cells fluctuate significantly more than primary cancer cells. Our study shows the potential of IPM for aiding in diagnosis and monitoring of cancer and other diseases.

ACKNOWLEDGMENTS

REFERENCES

[1] Shaked, N. T., Satterwhite, L. L., Rinehart, M. T., and Wax, A., [Holography, Research and Technologies], J. Rosen (Ed.), InTech, 219-236 (2011).

[2] Shaked, N. T., Satterwhite, L. L., Truskey, G. A., Telen, M. J., and Wax, A., "Quantitative microscopy and nanoscopy of sickle red blood cells performed by wide field digital interferometry," Journal of Biomedical Optics Letters 16(3), 030506:1-3 (2011).

[3] Bishitz, Y., Gabai, H., Girshovitz, P., and Shaked, N. T., "Optical-mechanical signatures of cancer cells based on fluctuation profiles measured by interferometry," Accepted to Journal of Biophotonics (2013).

[4] Girshovitz, P., and Shaked, N. T., "Compact and portable low-coherence interferometer with off-axis geometry for quantitative phase microscopy and nanoscopy," Optics Express 21(5), 5701-5714 (2013).

[5] Gabai, H., and Shaked, N. T., "Dual-channel low-coherence interferometry and its application to quantitative phase imaging of fingerprints," Optics Express 20(24), 26906-26912 (2012).

[6] Shaked, N. T., "Quantitative phase microscopy of biological samples using a portable interferometer," Optics Letters 37(11), 2016-2019 (2012).

[7] Girshovitz, P., and Shaked, N. T., "Generalized cell morphological parameters based on interferometric phase microscopy and their application to cell life cycle characterization," Biomedical Optics Express 3(8), 1757-1773 (2012).

[8] Park, Y-.K., Diez-Silva, M., Popescu, G., Lykotrafitis, G., Choi, W., Feld, M. S., and Suresh, S., "Refractive index maps and membrane dynamics of human red blood cells parasitized by Plasmodium falciparum," PNAS 105(37), 13730-13735 (2008).

[9] Cross, S. E., Jin, Y-S., Rao, J., Gimzewski, J. K., "Applicability of AFM in cancer detection," Nature Nanotechnology 4, 72-73 (2009).

[10] Swaminathan, V., Mythreye, K., O'Brien, E. T., Berchuck, A., Blobe, G. C., and Superfine, R., "Mechanical stiffness grades metastatic potential in patient tumor cells and in cancer cell lines," Cancer Research 71, 1-6 (2011).

[11] Bhadriraju, K., and Hansen, L. K., "Extracellular matrix- and cytoskeleton-dependent changes in cell shape and stiffness," Experimental Cell Research 278(1), 92-100 (2002).

[12] Bao, G., and Suresh, S., "Cell and molecular mechanics of biological materials," Nature Materials 2, 715-725 (2003).

[13] Suresh, S., "Biomechanics and biophysics of cancer cells," Acta Biomaterialia 3, 413-438 (2007).

[14] Arber, N., Sutter, T., Miyake, M., Kahn, S. M., Venkatraj, V. S., Sobrino, A., Warburton, D., Holt, P. R., and Weinstein, I. B., "Increased expression of cyclin D1 and the pRB tumor suppressor gene in c-K-Ras transformed Rat enterocytes," Oncogene 12, 1903-1908 (1996).

[15] Arber, N., Han, E. K. H., Sgambato, A., Piazza, G. A., Delohery, T. M., Begemann, M., Weghorst, C. M., Kim, N. H., Pamukcu, R., Ahnen, D. J., Reed, J. C., Weinstein, I. B., and Holt, P. R., "A K-ras oncogene increases resistance to Sulindac-induced apoptosis in rat enterocytes," Gastroenterology 113, 1892-1900 (1997).

[16] Kazanov, D., Dvory-Sobol, H., Pick, M., Liberman, E., Strier, L., Choen-Noyman, E., Deutsch, V., Kunik, T., and Arber, N., "Celecoxib but not Rofecoxib inhibits the growth of transformed cells in vitro," Clinical Cancer Research 10, 267-271 (2004).

[17] Sagiv, E., Memeo, L., Karin, A., Kazanov, D., Jacob–Hirsch, J., Mansukhani, M., Rechavi, G., Hibshoosh, H., and Arber, N., "CD24 is a new oncogene, early at the multistep process of colorectal cancer carcinogenesis," Gastroenterology 131, 630-639 (2006).

[18] Zipin-Roitman, A., Meshel, T., Sagi-Assif, O., Shalmon, B., Avivi, C., Pfeffer, R. M., Witz, I. P., and Ben-Baruch, A., "CXCL10 promotes invasion-related properties in human colorectal carcinoma cells," Cancer Research 67, 3396-3405 (2007).

[19] Kubens, B. S., and Zänker, K. S., "Differences in the migration capacity of primary human colon carcinoma cells (SW480) and their lymph node metastatic derivatives (SW620)," Cancer Letters 131, 55-64 (1998).